Journal of Applied Mechanics and Technical Physics, Vol. 41, No. 3, 2000

RELAXATIONAL EFFECTS IN THE DYNAMICS OF GROUNDS AND ROCKS

A. V. Mikhalyuk and V. V. Zakaharov

UDC 539.376 + 624.131

The specific features of the mechanical behavior of geophysical media (grounds and rocks) connected with their relaxation upon dynamic loads are analyzed. The influence of the intensity, nonuniformity, and rate of loading and the phase compositions of the media on the development and anisotropy of relaxational processes is shown. The existence of three mechanisms of relaxation, namely, viscous, structural, and migration (filtration) mechanisms, is shown.

It is known that any macroscopic physical system (gases, liquids, or solids) passed from the state of thermodynamic equilibrium under the action of one factors or another (pressure, temperature, etc.) tends toward restoring the equilibrium state (relaxes). Geophysical media such as grounds and rocks subjected to a broad spectrum of force, thermal, and other actions with time intervals from microseconds to geological epochs are not an exception.

As an object of engineering activity, grounds and rocks undergo mainly mechanical loads; therefore, great attention (see, e.g., [1]) has been paid to the specific features of their deformation and fracture (including phenomena connected with relaxational processes). In slow (static) loading regimes, the decrease in stresses upon fixed deformation, the delay of strains relative to the level of loading, the increase in the rate of equilibrium restoring with temperature rise, etc., occurs owing to relaxation. However, a number of phenomena that are due to relaxational processes were observed at dynamic loads as well: the increase in strains after the onset of unloading from stresses [2], the dependence of the strain characteristics and the strength on the loading (strain) rate [3, 4], a hysteresis-like form of ground [5] and rock [6] dynamic-deformation diagrams, the existence of very different limiting deformation diagrams (dynamic as $d\sigma/dt \to \infty$ and static as $d\sigma/dt \to 0$) [5], and the dynamic aftereffect (unloading from deformations after complete unloading from stresses) [6]. At the same time, some features of the behavior of grounds and rocks, which are connected with relaxation and permit one to study the possible mechanisms (first of all, in dynamic loading), have not been embodied in the literature. Below, their description is given on the basis of experimental studies of the dynamic deformation of two, essentially different classes of geophysical media, namely, soft high-porosity, readily compressible grounds of various phase composition (loams and clays) and hard rocks of insignificant porosity and humidity or monolithic rocks (aleurolites, anhydrites, argillites, granites, dolomites, limestones, rock salt, coal, sandstone, shell rocks, and ampelite).

The total number of dynamic-deformation experiments on geophysical media with variation from a uniaxial stress state to all-round uniform deformation is 214; 72 experiments with grounds and 142 with solid and semisolid rocks were performed. In addition, experiments with model materials with very different mechanisms and rates of relaxational processes, namely, with metals (lead, steel, aluminum, and D-16T duralumin), liquid (spindle oil), artificial materials (concrete and cast mica), polymers (polymethylmethacrylate), and ice, were performed. These experiments are 42 in number.

Institute of Geophysics, National Academy of Sciences, Kiev 02054, Ukraine. Translated from Prikladnaya Mekhanika i Tekhnicheskaya Fizika, Vol. 41, No. 3, pp. 202–212, May–June, 2000. Original article submitted February 16, 1999.

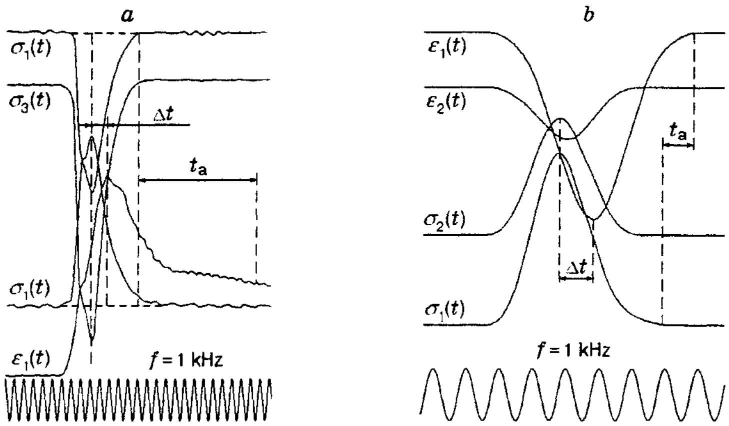

Fig. 1

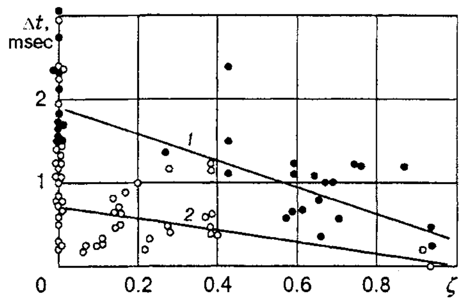

Fig. 2

Some specific features of the development of relaxational processes that affect the experimental technique are noteworthy.

1. Strictly speaking, the time at which the thermodynamic equilibrium is established (especially in such slowly relaxing systems as geophysical media) is very great, because the closer the system to the state of equilibrium, the slower it restores. In other words, an infinitesimal deviation from the state of equilibrium requires an indefinitely large time for restoring of this state. It is almost impossible to perform such measurements; therefore, in the experiments described below, the development of relaxational processes was studied in the intervals limited by the resolving power of an experimental setup ($t \geqslant 10^{-5}$ sec).

2. Because, upon loads occurring in engineering practice, the grounds and rocks behave like barotropic media [2], the temperature variation was not taken into account in analysis of relaxational processes.

The experiments with grounds were performed by the technique described in [5], and those dealing with dynamic deformation of rocks by the technique given in [7].

The ground samples were subjected to dynamic tests under the conditions of a simple deformed state: $\sigma_1(t) > \sigma_2(t) = \sigma_3(t) = \zeta\sigma_1(t) > 0$ (ζ is the lateral-pressure coefficient) for $\varepsilon_1(t) > \varepsilon_2(t) = \varepsilon_3(t) = 0$, and the rock and model-material samples were tested under the conditions of uniaxial $[\sigma_1(t) > \sigma_2(t) = \sigma_3(t) = 0]$ or triaxial $[\sigma_1(t) > \sigma_2(t) = \sigma_3(t) > 0]$ compression.

The amplitude–time characteristics of dynamic loading (σ_1^m is the amplitude of the largest principal stress σ_1, t_{inc} is the time of stress increase σ_1, and t_+ is the total time of pulse-pressure action) were varied in quite a broad range:

— for grounds, we have $\sigma_1^m = 1.8$–14.5 MPa, $t_{\text{inc}} = 1.40$–9.39 msec, and $t_+ = 3.28$–21.10 msec;

— for rocks, we have $\sigma_1^m = 1.99$–1130 MPa, $t_{\text{inc}} = 0.242$–12.97 msec, and $t_+ = 1.97$–28.54 msec;

— for model materials, we have $\sigma_1^m = 64.0$–408.7 MPa, $t_{\text{inc}} = 1.14$–3.48 msec, and $t_+ = 2.40$–6.75 msec.

The relaxational character of the development of dynamic deformation follows from the oscillograms of the signals $\sigma_1(t)$, $\sigma_2(t) = \sigma_3(t)$, $\varepsilon_1(t)$, and $\varepsilon_2(t) = \varepsilon_3(t)$ shown in Fig. 1 for uniaxial compression of a yellow-green clay of disordered structure with 28.8% humidity (a) and triaxial compression of a rock salt (b). Above all, this is indicated by the phase shift (time lag) of strains relative to stresses Δt, which can be equal to a few milliseconds. The results of solid-rock experiments with varied nonuniformity of dynamic loading show that the phase shift between stresses and strains in geophysical media depends on the deformation pliability (rigidity and strength) and the nonuniformity of loading. Figure 2 shows the phase shift vs. the nonuniformity of loading, which is characterized by the ratio between the smallest and largest principal stresses $\zeta = \sigma_3/\sigma_1$ for two groups of rock with approximately identical properties:
hard rocks with strength $\sigma_0 > 75$ MPa upon uniaxial compression [limestones, dolomites, ampelite, sand stones, aleurolites, argillites, and granites (open points)]; soft rocks with $\sigma_0 \leqslant 30$ MPa [coal, shell rocks, etc. (filled points)]. Despite the significant scatter of the values of Δt for each group, which is due to the different properties of separate varieties of mineral formations and the influence of random factors (such as nonconstant amplitudes and loading rates), one can distinguish two specific features of this dependence, which are important for clarifying the mechanisms of relaxational processes in rocks:

— The phase shift of strains increases with the nonuniformity of loading;

— In media of great deformation pliability (i.e., capable of sustaining more intense structural changes), the phase shift of strains is a factor of 2.5–4 greater than in hard rocks with mainly the elastic development of deformation.

With such a significant scatter of experimental data, it is difficult to propose quite a justified approximation of the correlation between Δt and ζ; in the first approximation (within the range $0 \leqslant \zeta \leqslant 1$), one can present it in the form $\Delta t = 0.7(1 - \zeta)$ (curve 2 in Fig. 2) and $\Delta t = 1.6(1.19 - \zeta)$ (curve 1). These dependences show that as the stress state approaches the all-round uniform compression, the phase shift of strains in hard rocks almost disappears; in soft rocks, for $\zeta = 1$ the quantity Δt differs noticeably from zero. Similar dependences $\Delta t(\zeta)$ hold for polymer materials. In particular, for uniaxially compressed polymethylmethacrylate, the phase shift of strains reaches 0.24–1.04 msec; however, as the nonuniformity of the stress state is reduced, the quantity Δt rapidly decreases to 0.056–0.117 msec for $\zeta \approx 0.4$–0.5. In the experiments with model materials such as spindle oil, lead, aluminum, duralumin, and steel, the phase shift between strains and stresses was not observed.

In rocks, the phase shift of strains relative to stresses is much more significant than in other media; this indicates that the rate of relaxational processes in geophysical media is small (and, hence, the relaxation times are large). One can draw this conclusion if one takes into account that upon intense loading of continuous media that are capable of relaxing, the relations

$$\eta_1 \approx G\tau, \qquad \eta_2 \approx K\tau \tag{1}$$

hold. Here η_1 and η_2 are the shear and volume viscosities of the medium, respectively, and G and K are the moduli of shear and volume elasticity, respectively [8].

As applied to rocks, which are structured media, the calculation by formulas (1) gives the lower estimate of the relaxation time, since they also have another (in addition to the viscous mechanism) mechanism of relaxational processes which promote the increase in the total relaxation time. Using the data on the deformation properties and viscosity of rocks upon corresponding loading regimes (see, e.g., [7]), one can find that the lower limit τ has an order of 10^{-3} sec, i.e., it coincides in order of magnitude with the quantity Δt.

The phase shifts between the stress- and strain-tensor components are different. The time lag of $\varepsilon_1(t)$ behind $\sigma_1(t)$, i.e., in the direction of action of the maximum principal stress, is the largest. In grounds and rocks, the time lag can vary from 0.15–0.20 to 3.0–3.5 msec. The phase shift of the transverse strains is much smaller: it does not exceed 1–2 msec relative to σ_1^m and 0–0.1 msec relative to σ_2^m. Thus, the anisotropy of relaxational processes is inherent in rocks: in the directions of action of the strains σ_2 and σ_3, the relaxational processes occur much more rapidly than in the direction of σ_1, despite the fact the absolute values of ε_2 and ε_3 can be comparable and even exceed [9] the strain ε_1 owing to dilatant phenomena at a comparatively large nonuniformity of the stress state. This is manifested most distinctly at uniaxial dynamic loading of rocks. It is noteworthy that the anisotropy of relaxational processes is not connected with the genetic anisotropy of the properties of rocks and is observed in media which may be considered isotropic (massive homogeneous sandstone, rock salt, granite, etc.).

In the majority of experiments, phase shifts between separate stress-tensor components were not observed; however, in some cases, a weak time lag of σ_2 behind σ_1 (in amplitudes) occurs. It can reach 40–50 μsec in carbonite rocks, 88 μsec in sandstones and aleurolites, 400 μsec in rock salts, 13 μsec in polymethylmethacrylate, 148 μsec in cast mica, and 6 μsec in metals. On average, in the experiments, the time displacement between σ_1 and σ_2 varies from 1.4 to 26 μsec in different media. In rock salts, it reaches 92.2 μsec.

Deceleration of the relaxational processes in rocks with increase in the nonuniformity of their stress states allows one to conclude that relaxation in these media is connected not only with viscosity [5] but also with deformation-induced structural changes. Since the nonuniformity of loading promotes the onset and development of structural imperfection (caused, in particular, by dilatancy [10]) in a deformable medium, one can assume that this deceleration is connected with greater micro and macrocracking owing to intercrystalline or intracrystalline sliding [11].

We assume that upon irregular dynamic loading (uniaxial compression), the deformation is accompanied by dilatant loosening of the rock structure according to Stavrogin's model [12], i.e., the increase in the specimen volume is a consequence of the formation of internal ruptures and shear sites. Local stress concentrations which relax in the formation of sliding planes arise around these structural defects. Because these defects arise mainly uniformly over the entire deformed volume [7, 10] during dilatant processes, the duration of sliding-plane (microcrack) propagation should be comparable with the time of strain delay (relative to stresses). Since the data on the velocity V_* of similar defects in rocks are lacking, for an approximate estimate, we use the fact that the fracture velocity of the cross connections between the structural defects is approximately 5–10% of the maximum microcrack velocity in the medium [13]. Its dependence on the elastic properties of the medium subjected to deformation can be obtained from the Poncelet dependence [14] of the crack-growth rate on the elastic-wave velocity V_p. Then,

$$V_* = (0.05\text{–}0.1)V_p\sqrt{\frac{1-2\nu}{2(1-\nu)}}.$$

For rocks, we have $V_* = 86\text{–}257$ m/sec.

According to Stavgorin's dilatancy model, for the specimens used in the experiments ($d \approx 4$ cm and $h \approx 7.5$ cm), the total maximum length of the lines of sliding on the specimen height is approximately 13 cm, and the duration of its formation is of the order of $(0.51\text{–}1.51)\cdot 10^{-3}$ sec; this almost coincides with the phase shift between stresses and strains upon uniaxial compression, when intense dilatant loosening of the rock structure occurs. This estimate allows us to conclude that the delay of strains can be connected not only with the viscous, but also with the structural reorganization of the medium. This conclusion is supported by the change in the shape of the pressure pulse with increased nonuniformity of the stress state in the rock specimen. If the ratio of the time of pressure rise $t_{\rm inc}$ to the total time of pulse action t_+ is 0.36–0.40 upon dynamic loadings as $\zeta \to 0$, the pulse acquires an almost symmetric shape ($t_{\rm inc}/t_+ = 0.50\text{–}0.55$) in stress states close to all-round uniform compression ($\zeta \to 1$). Thus, upon loading with high nonuniformity, the unloading time, when the structural changes occur in the medium subjected to deformation, is a factor of 1.5 greater than upon uniform loading.

In the grounds that are three-phase systems, in which each phase plays an important role in the development of deformation, the time lag of strains depends greatly on their phase structure and the loading regime. Figure 3a shows the quantity Δt vs. the loading rate $\dot{\sigma}_1$. Curve 3 is plotted on the basis of the experimental results obtained for grounds with 13–15% humidity, curve 1 for loams (9.6% humidity), and curve 2 for a clay (23.5% humidity). It follows from Fig. 3 that the phase shift of strains reaches the largest values upon dynamic loading with a small rate of pressure rise (in all the experiments, attention was paid to the inadmissibility of drainage of the pore moisture, i.e., the moisture content of the ground was preserved).

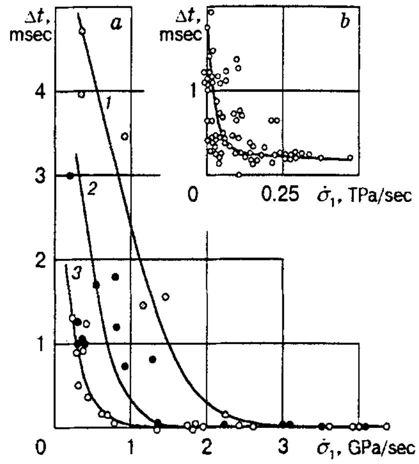

Fig. 3

An increase in the loading rate results in a rapid decrease in the delay of strains; for certain finite values of $\dot{\sigma}_1$, the phase shift of strains almost disappears. We note that this critical dynamic-loading rate almost coincides with the quantity which corresponds to reaching the ultimate dynamic compression diagram by the deformation process, which, according to [15], is 1.3–1.5 GPa/sec for light brown loams (14.17% humidity), 2.8–3.0 GPa/sec for loams (9.63% humidity), 3 GPa/sec for yellow-green clays, 2.0–2.2 GPa/sec for green clays (23.5% humidity), and approximately 4 GPa/sec for green clays (15% humidity). Thus, it follows from Fig. 3a that the phase shift between stresses and strains is observed in nonlimiting loading (deformation) regimes. The viscous effects of deformation are manifested most distinctly precisely in this region [2].

The dependence $\Delta t(\dot{\sigma}_1)$ is characteristic of solid rocks as well (Fig. 3b). Despite the significant scatter of experimental data, for most rocks this dependence holds for loading rates up to 100–200 GPa/sec, i.e., two orders of magnitude greater than for grounds. However, these loading rates are not limiting dynamic rates, because a non-zero phase shift of strains relative to stresses is preserved for them. As can be seen from Fig. 3b, the tendency toward decreasing Δt with further increase in the loading rate is preserved; however, we failed to reach this loading regime in solid rocks for $\Delta t \approx 0$.

The results in Fig. 3a show that the rates of relaxational processes depend on the relations between the phases of grounds. If the humidity of a ground is small, the deformation process has a character of structural reorganization of the skeleton with overcoming of "dry"-friction forces between the mineral grains. This requires significant energy expenditures and, with other things being equal, is accompanied by deceleration of deformations. An increase in humidity results in a decrease in the power consumption of ground deformation and an increase in the strain rate [5, 15, 16]. However, as a free moisture capable of migrating in the porous space appears, the structural reorganization in a ground subjected to loading is accompanied by local migration which promotes the equalization of the stress state between separate phases of the ground in its volume and slows down the relaxational processes (as was noted above, in dynamic loading the ground specimen deforms according to the closed drainage-free scheme). This occurs until the ground structure contains porous regions into which the porous moisture can migrate under the action of internal pressure gradients. One can assume that at quite a high humidity, when the state of the ground approaches the state of "ground mass " (i.e., when the free porosity is small or absent), the ground deforms like a liquid in which the rate of relaxational processes is great and is determined only by its viscosity. In this case, the phase shift of strains is so small that for a resolving power of the experimental complex of 10^{-5} sec, it cannot affect the strain oscillograms.

Thus, in dynamic loading there should be at least three relaxation mechanisms, namely, structural, viscous, and migration (filtration) mechanisms, in the ground. The role of one mechanism or another depends on the phase structure of the ground. In low-humidity grounds with large free porosity, the main role in the development of the processes is played by the structural mechanism (as in solid rocks). In grounds with a humidity sufficient to play the role of effective intergrain "lubrication " but inadequate for the appearance of a free liquid capable of migrating under the action of contact pressure gradients and such that the ground becomes a "ground mass" (i.e., an aqueous-mineral mixture that does not resist shear), the viscous mechanism of relaxation dominates, at which the rates of relaxational processes are maximum. If the phase structure of a ground is such that, together with free moisture, there is also free porosity, the rates of relaxational processes are affected by migration of a free unbounded liquid.

Figure 4 shows the dependence of the phase shift of strains in yellow-green clays on their humidity (curve 2). The behavior of the curve confirms the above remarks. The first minimum of the phase shift is observed for a humidity of clays in the range 10–15%; this corresponds to the amount of moisture determined by saturation of the adsorption films of mineral grains [5]. The decrease in the humidity of the ground is accompanied by an increase in the phase shift. A similar phenomenon is observed for $w > 15\%$; however, in this area, the quantity Δt increases until the ground humidity reaches 25–26%; after that, Δt rapidly decreases.

The so-called *dynamic aftereffect* is a bright manifestation of relaxational processes in grounds and rocks. This process can last quite long: up to 15–18 msec in clay grounds and permafrost, 10–11 msec in sandstones, 12–20 msec in limestones, 16.3 msec in anhydrites, 17 msec in aleurolites, and 12.5 msec in salts. However, in most cases, the dynamic aftereffect is significantly weaker in solid rocks than in grounds and does not exceed 2–5 msec. The experimental results show that, in practice, the dynamic-aftereffect period t_a does not depend on the nonuniformity of the stress state in the medium, which does not contradict the physical nature of the effect considered. It is noteworthy that the dynamic aftereffect (and the phase shift of strains as well) is considerable in the direction of action of the largest principal stress σ_1 (with which the majority of originating defects of the structure are connected) and is practically absent in the direction of action of the smallest principal stress.

In grounds, the duration of elastic unloading from deformations after complete unloading from stresses depends on the phase structure of the ground, and this dependence is similar to that considered above $\Delta t(w)$ (curve 1 in Fig. 4). For low humidity of a ground, the elastic unloading decelerates owing to overcoming of friction forces during intergrain sliding; for $w_{\text{ad}} < w < w_{\text{tot}}$ (w_{ad} is a humidity that corresponds to saturation of the adsorption films of ground particles and $_{\text{tot}}$ is a humidity that corresponds to the total moisture content of the ground), the motion of the ground moisture when the entrapped and compressed gas (air) expands affects the elastic unloading.

The phase shift of strains and the aftereffect are reflected in the dynamic-deformation diagrams of grounds and rocks, which have a hysteresis-like form [2, 5, 7]. Its correlation with relaxational processes is obvious. In fast dynamic processes in relaxing media, the equilibrium deformation has no time to develop during loading; therefore, at the stage of pressure rise, the deformation diagram displaces toward the side of deformation reduction (toward the stress axis). This displacement is the larger, the greater the loading (strain) rate and the slower the relaxational processes in the medium. In dynamic unloading, the deformation also lags behind the equilibrium values (because of the delay of the reversible component); however, in this case, the equilibrium deformation should be smaller than the registered deformation, i.e., the diagram of $\sigma(\varepsilon)$ displaces toward the side of deformation intensification (from the stress axis). With reduction of the dynamic character of the deformation process, the effects of delay degenerate; the loading and unloading branches approach each other and coincide upon static deformation [6] (if the level of loading does not cause plastic deformations).

As follows from the experiments, the increase in ε_1 in solid rocks can proceed as σ_1 decreases to 42% in sandstones, 40% in granites, 38% in aleurolites, 49% in limestones, 55% in dolomites, 60% in salts, 68% in shell limestones, 22% in concrete, and 47% in polymethylmethacrylate. In the absence of the phase shift of strains, the unloading from deformations begins simultaneously with unloading from stresses, although the hysteresis-like character of the deformation diagrams is preserved. It follows from the above data that

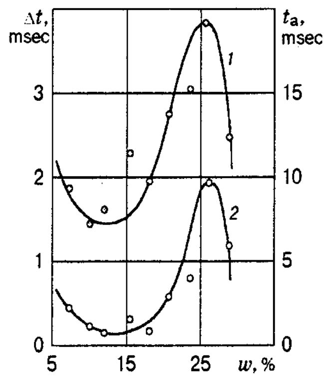

Fig. 4

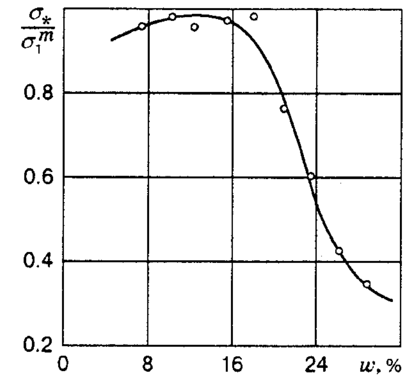

Fig. 5

this effect in soft rocks is manifested more strongly than in hard rocks. The transverse strain ε_2 reacts more rapidly to a change in the stress-state intensity: its increase ceases even when σ_1 decreases by approximately 22.2%; in many cases, the unloading from ε_2 begins simultaneously with unloading from σ_1. This also points to the anisotropy of the rates of relaxational processes in rocks.

In grounds, the unloading from deformations depends on the loading intensity and the phase structure. Upon intense loading with rates close to the limiting rates, the unloading from deformations begins simultaneously with unloading from stresses. In nonlimiting regimes, the maximum strains are observed when the loading intensity decreases to a certain value of σ_* determined by the ground humidity. This dependence is plotted in Fig. 5 for structurally disordered clays with 7.5–28.8% humidity with a constant density of the skeleton of $1.63 \cdot 10^3$ kg/m^3.

It follows from Fig. 5 that the structural mechanism exerts a weaker effect on the relaxational processes in grounds than in solid rocks: in the range of humidities of up to $w = 16$–18%, the unloading from deformations begins almost simultaneously with unloading from stresses: $\sigma_* \leqslant (0.96\text{–}0.99)\sigma_1^m$. With appearance of free moisture, the deceleration of deformation intensified rapidly. As $w \to w_{\rm tot}$, the maximum deformations were observed for $\sigma_* = 30$–35% of the loading amplitudes.

Many attempts were undertaken to describe the behavior of grounds and rocks as media that are capable of relaxing. As a rule, they were based on the models of media with the viscous mechanism of relaxation. According to [2], the hysteresis-like character of the diagrams and the more intense deformations on the unloading-from-stress branch can be described by the equation of a viscoelastic body with various static- and dynamic-deformation diagrams:

$$\mu\varepsilon(t) + \dot{\varepsilon}(t) = \frac{1}{E_{\rm dyn}}\,\dot{\sigma}(t) + \frac{\mu}{E_{\rm st}}\,\sigma(t). \tag{2}$$

Here $E_{\rm dyn}$ and $E_{\rm st}$ are the limiting dynamic and static moduli of elasticity, respectively, $\mu = E_{\rm dyn}E_{\rm st}[\eta(E_{\rm dyn} - E_{\rm st})]^{-1}$, and η is the coefficient of dynamic viscosity of rock (ground).

To assess the applicability of the model of a viscoelastic body to the description of deformation processes in real rocks, we use the method of constructing deformation diagrams for a concrete experiment given in [2]. To do this, it is necessary to specify the pressure pulse $\sigma(t)$, find the time history of the strain $\varepsilon(t)$ from Eq. (2), and construct the diagram $\sigma(\varepsilon)$ with the time excluded.

Taking into account that the form of the pressure pulse is close to symmetric (see. Fig. 1), we specify the stresses in the form

$$\sigma(t) = A\sin(\omega t) = A\sin\frac{2\pi t}{T}, \tag{3}$$

where A is the loading, ω is the circumferential frequency ($0 \leqslant \omega t \leqslant \pi$), and T is the period of the oscillatory process. Substituting (3) into (2), we obtain

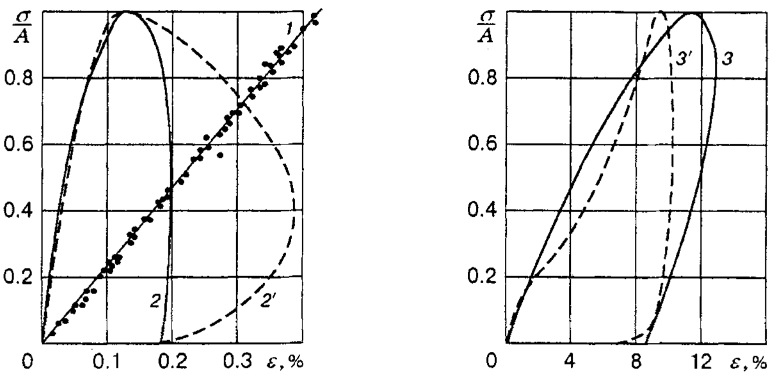

Fig. 6

$$\mu\varepsilon + \dot{\varepsilon} = a\cos(\omega t) + b\sin(\omega t), \qquad a = \frac{A\omega}{E_{\text{dyn}}}, \qquad b = \frac{A\mu}{E_{\text{st}}}.$$

This equation is the first-order linear equation whose general solution has the form

$$\varepsilon(t) = \exp\Big(-\int \mu\,dt\Big)\Big[\int \exp\Big(-\int \mu\,dt\Big)(a\cos(\omega t) + b\sin(\omega t))\,dt + C\Big], \tag{4}$$

where C is an integration constant. We integrate Eq. (4) with allowance for $\int \mu\,dt = \mu t$. The integration constant is found from the condition $\varepsilon(t) = 0$ for $t = 0$. As a result, we obtain

$$\varepsilon(t) = \frac{1}{\mu^2 + \omega^2}\,[(a\omega + b\mu)\sin(\omega t) + (a\mu - b\omega)(\cos(\omega t) - \exp(-\mu t))]. \tag{5}$$

Discarding the time t from (3) and (5), we derive the equation of deformation diagram

$$\varepsilon(\sigma) = \frac{1}{\mu^2 + \omega^2}\Big\{(a\omega + b\mu)\frac{\sigma}{A} + (a\mu - b\omega)\Big[\sqrt{1 - \frac{\sigma^2}{A^2}} - \exp\Big(-\frac{\mu}{\omega}\arcsin\frac{\sigma}{A}\Big)\Big]\Big\}. \tag{6}$$

Formula (6) was used to plot the dynamic-deformation diagram of a model material, spindle oil in this case (curve 1 in Fig. 6); points refer to the results of the loading experiments in the range $\sigma_1 = 77.8$–85.5 MPa, $t_{\text{inc}} = 2.71$–3.54 msec, and $t_+ = 4.60$–6.49 msec.

Figure 6 shows that formula (6) describes satisfactorily the mechanical behavior of the medium upon dynamic loading. Owing to the low viscosity and the large rate of relaxation, the loading and unloading branches coincide; moreover, the dynamic compressibility of the oil coincides with the certificate (static) compressibility, which is characteristic of liquids.

Curves 2 and 3 in Fig. 6 refer to dynamic-deformation diagrams for a rock (rock salt) and a ground (Kerch green clay having a 23.5% humidity), which were plotted according to formula (6). For the rock, we have $\sigma_1^m = A = 9.1$ MPa, $T = 8$ msec, $\omega = 785.4$ sec^{-1}, $E_{\text{st}} = 3.8$ GPa, $E_{\text{dyn}} = 26.79$ GPa, and $\eta = 8.5$ MPa·sec; for the ground, we have $\sigma_1^m = A = 5$ MPa, $T = 14.4$ msec, $\omega = 436.1$ sec^{-1}, $E_{\text{st}} = 28.8$ MPa, $E_{\text{dyn}} = 71.5$ MPa, and $\eta = 0.196$ MPa · sec. Curves 2′ and 3′ refer to experimental diagrams. One can see satisfactory agreement between the theoretical and experimental diagrams only at the stage of loading, where the maximum divergences between them do not exceed 15–17% in solid rocks and 25% in grounds (the more significant differences between the diagrams of ground deformation at the stage of loading are connected with the adopted approximation of the pressure pulse whose shape is a distinct bell in grounds rather than a semi-sinusoid). The unloading branches of the theoretical and experimental diagrams differ greatly. It is noteworthy that, for rock salts, the maximum deformation on the theoretical and experimental diagrams is attained when the stress in the medium is approximately 40% of the pressure-pulse amplitudes; although their values differ by almost a factor of 1.9–2.0. At the same time, the deformations that correspond to the moment of complete unloading from stresses, i.e., the aftereffect deformations, coincide with an error of up to 6.1%. The distinctions in the forms of the unloading branches of solid rocks allow us to conclude that the deformation process is determined not only by the elastic and viscous mechanisms (as follows from the equation of state of the medium), but also other mechanisms of deformation primarily connected with the structural rearrangement (see [6]).

For grounds, the maximum deformation is reached for $\sigma/A = 0.85$ on the theoretical diagram and at a stress equal to 60–80% of the pressure-pulse amplitudes on the experimental curve. In the range of small stresses ($\sigma \leqslant 0.2A$) the unloading branches on the theoretical and experimental diagrams almost coincide (the divergence is not greater than 4%); we note that the aftereffect deformations differ only by 19.2%. Nevertheless, the general view of the experimental unloading branch shows that in a ground with such a phase structure, the deformation process at the stage of unloading occurs more rapidly and requires smaller energy expenditures compared to the model expenditures. Probably, this is connected with the fact that because of the small structural strength of grounds, upon deformation their structure rearranges mainly at the stage of loading rather than unloading. In grounds with a humidity close to the complete moisture saturation, the unloading branch becomes similar to that described for solid rocks (see, e.g., [7]); the difference in the magnitude of deformations increases by a factor of 2.5–3, which can be connected with the effect of migration of the intraporous moisture.

Thus, the relaxational effects in the dynamics of grounds and rocks depend on relaxation mechanisms the most prominent of which are viscous, structural, and migration (filtration) mechanisms. Allowance for these mechanisms is necessary not only in analysis of theoretical problems of ground and rock mechanics, but also in developing pulse technologies of action on similar media.

REFERENCES

1. N. V. Ornatskii, *Mechanics of Grounds* [in Russian], Izd. Mosk. Univ., Moscow (1962).
2. G. M. Lyakhov and N. I. Poluakova, *Waves in Dense Media and Loads on Structures* [in Russian], Nedra, Moscow (1967).
3. A. N. Stavrogin and E. D. Pevzner, "Physicomechanical properties of rocks upon dynamic loads under the conditions of complex stress states," in: *Physical Properties of Rocks for Large Thermodynamic Parameters* [in Russian], Naukova Dumka, Kiev (1971), pp. 204–206.
4. G. M. Kryukov and M. G. Gorbonos, "Delay of fracture and increase in rock strength upon dynamic loading," *Fiz. Tekh. Probl. Razrab. Polezn. Iskop.*, No. 1, 41–47 (1978).
5. A. A. Vovk, B. V. Zamyshlyaev, L. S. Evterev, et al., *Behavior of Grounds under the Action of Pulse Loads* [in Russian], Naukova Dumka, Kiev (1984).
6. A. V. Mikhalyuk and V. V. Zakharov, "Dissipation of dynamic-loading energy in quasi-elastic deformation processes in rocks," *Prikl. Mekh. Tekh. Fiz.*, No. 2, 162–169 (1997).
7. A. V. Mikhalyuk, *Rocks in Nonuniform Dynamic Loading* [in Russian], Naukova Dumka, Kiev (1980).
8. L. D. Landau and E. M. Lifshits, *Continuum Mechanics* [in Russian], Gostekhteoretizdat, Moscow (1954).
9. A. V. Mikhalyuk and V. V. Zakharov, "Relaxational phenomena in rocks upon dynamic loads," *Fiz. Tekh. Probl. Razrab. Polezn. Iskop.*, No. 4, 3–13 (1998).
10. L. Obert, in: *Fracture*, Vol. 7: *Fracture of Nonmetals and Composites*, Academic Press, New York–London (1972).
11. I. V. Luchitskii, V. I. Gromin, and G. D. Ushakov, *Rock Deformation Experiments at High Pressures and Temperatures* [in Russian], Nauka, Novosibirsk (1967).
12. A. N. Stavrogin and A. G. Protosenya, *Plasticity of Rocks* [in Russian], Nedra, Moscow (1979).
13. V. M. Finkel', *Physics of Fracture* [in Russian], Metallurgiya, Moscow (1970).
14. Z. T. Bieniawski, "Fracture dynamics of rock," *Int. J. Fract. Mech.*, 4, No. 4, 415–430 (1968).
15. A. F. Lebedev, *Compaction of Grounds of Different Humidity* [in Russian], Stroivoenmorizdat, Moscow (1949).
16. R. L. Stavnitser, *Strains of the Bases of Structures in Shock Loading* [in Russian], Stroiizdat, Moscow (1969).